MAUSAM, 48, 3 (July 1997), 397-404

551.510.522 : 551.578.46

# A study of atmospheric boundary layer characteristics with ground snow cover - numerical method

N. RAMANATHAN and K. SRINIVASAN

*CAS, Indian Institute of Technology, New Delhi - 110016, India*

*(Received 15 May 1995, Modified 18 September 1996)*

**सार** — उपयुक्त संशोधनों के उपरान्त हिम आच्छादित धरातल पर वायुमंडलीय परिवर्तनों का अनुकरण करने के लिए एक - आयामी किस्म के मैसोस्केल मॉडल का प्रयोग किया गया है। सूक्ष्म और दीर्घ तरंग विकिरण पर मेघों के प्रभाव को सम्मिलित करने के लिए भी इस मॉडल में संशोधन किए गए हैं। इस मॉडल में हिमानी की ऊपरी परत तथा इसकी विभिन्न परतों, दोनों ही बिन्दुओं पर ऊष्मा संतुलन का पता लगाया गया है और यथा स्थानों पर बर्फ के पिघलने की दर का आकलन किया गया है। अनुरूपण के लिए श्रीनगर (कश्मीर) के शीत कालीन आँकड़ों का प्रयोग किया गया है। हिम पिघलन दर की दैनिक विभिन्नता और अन्य वायुमंडलीय विभिन्नताओं को मॉडल द्वारा एक साथ प्रदर्शित किया गया है। अनुभूत मानक फार्मूला के मानों के आधार पर पिघलन मानों की सत्यता का पता लगाया गया है। मॉडल द्वारा प्रदर्शित प्रक्षन्न, ताप विशिष्ट आर्द्रता और पवन गति की पार्श्व स्थिति उपलब्ध प्रेक्षणों के साथ युक्ति संगत रूप से अनुरूप पाई गई है। भूतल कर्ष्ण गुणांक के परिवर्तनों से संबंधित परिणाम असंवेदी पाए गए हैं।

**ABSTRACT**. A one-dimensional version of a mesoscale model was used to simulate the atmospheric variables over ground snow cover after incorporating suitable modifications. Modifications to include the effect of cloud on shortwave and longwave radiation were also made in the model. The model takes into account both the heat balance at the snow surface and at various layers of the snow pack and calculates the melt rate *in situ*. Srinagar (Jammu & Kashmir) winter data was used for the simulations. The diurnal variation of snowmelt rate and other atmospheric variables were simulated simultaneously by the model. Melt rate values were verified with the values obtained from standard empirical formula. The model-simulated profiles of potential temperature, specific humidity and wind speed were found to be in reasonable agreement with available observations. The results were found to be insensitive to changes in surface drag coefficients.

**Key words** — Atmospheric Boundary Layer (ABL), Model simulation, Shear zone, Snow melt rate.

## 1. Introduction

Snow cover is long known to influence the seasonal weather and climate of a region. Various studies are available in literature relating to air-snow interaction. The models developed by hydrologists mainly concentrate on the effect of changing atmospheric conditions on the melting or run-off in a snow pack (Anderson 1976) and little is said about the influence of snow on the atmosphere. Granger and Male (1978), McKay and Thurtell (1978) among others have carried out some observational studies on air-snow interaction.

However, these studies were confined to the first few metres above the snow cover. Kondo and Yamazaki (1990) developed a heat balance model to calculate the snow-melt and snow temperature including phase changes of snow. However, the effect of snow cover on the atmospheric variables was not studied.

Meteorologists are generally concerned about the influence of snow on the atmospheric variables. Halberstam and Melendez (1979), in their numerical study, reported a strong relationship especially during nights, between the surface temperature and the bursts of turbulence which result from the frictional damping of surface layer winds during highly stable conditions. The *ad hoc* parameterization scheme used by them for simulating these were not described. Such occurrences of the bursts of turbulence were recorded by Schubert (1977) and Kahle *et al.* (1977) in their field observational studies using accoustic sounders.

Except for some observational studies (Upadhyay *et al.* 1981, Ohata *et al.* 1981), a comprehensive numerical study of the atmospheric boundary layer with ground snow cover has been unattempted so far in India. The purpose of this study is to simulate atmospheric variables with ground snow cover using a mesoscale model including phase changes of snow.

The model equations are given in section 2. Modifications made in the model are described in section 3. The initial data used alongwith boundary conditions are given in section 4. Results and conclusions are discussed in sections 5 and 6 respectively.

## 2. Model equations

A one-dimensional version of the University of Virginia Mesoscale Model was used for the present study after incorporating suitable modifications as discussed in the next section. This model was originally developed by Pielke (1974) and later on modified by Mahrer and Pielke (1977), McNider and Pielke (1981) etc. The 1-D model equations are :

$$\frac{du}{dt} = fv - fv_g + \frac{\partial}{\partial z}\left( k_z^m \frac{\partial u}{\partial z} \right)$$

$$\frac{dv}{dt} = -fu + fu_g + \frac{\partial}{\partial z}\left( k_z^m \frac{\partial v}{\partial z} \right)$$

$$\frac{d\theta}{dt} = \frac{\partial}{\partial z}\left( k_z^\theta \frac{\partial \theta}{\partial z} \right)$$

$$\frac{dq}{dt} = \frac{\partial}{\partial z}\left( k_z^q \frac{\partial q}{\partial z} \right) \qquad (1)$$

where, $\frac{d}{dt} = \frac{\partial}{\partial t} + w\frac{\partial}{\partial z}$

$u$ and $v$ are the components of wind velocity, $u_g$ and $v_g$ are the geostrophic wind components, $\theta$ and $q$ are the potential temperature and specific humidity respectively. $k_z^m, k_z^\theta$ and $k_z^q$ are respectively the eddy coefficients of momentum, heat and moisture. This atmospheric model was coupled with the snow melt model (discussed in the following section) developed by Kondo and Yamazaki (1990) and used in the present study.

## 3. Modifications

### 3.1. *Thermal heat balance over snow surface*

The model was originally developed for simulation of atmospheric variables over a bare soil surface. The surface energy balance equation was iteratively solved for surface temperature using Newton-Raphson technique at each time step. This is not applicable for a snow surface since the heat associated with the phase changes of snow also needs to be included. Moreover, snow being translucent to shortwave radiation, allows only a part of it to penetrate into the snow pack which often leads to melting of the inside layers even when the snow surface remains below freezing.

In the present study, the method given by Kondo and Yamazaki (1990) was used for calculating the snow pack temperature. At the snow surface it holds that,

$$C_s\rho_s \frac{\partial T_s}{\partial t}\Delta z = \lambda_s \left( \frac{\partial T}{\partial z} \right)_{z=0} + [\mu I \exp(-\mu z) - L_f F]\,\Delta z$$

$$+ \varepsilon_s R_L\downarrow - \varepsilon_s \sigma T_s^4 - H - LH \qquad (2)$$

The snow surface temperature ($T_s$) was obtained from the following differential form of Eqn. (2), *viz.*,

$$T_{n+1,1} = \frac{\lambda_s \Delta t}{C_s\rho_s(\Delta z)^2}(T_{n,2} - T_{n,1}) + \frac{\Delta t}{C_s\rho_s}$$

$$[\mu I \exp(-\mu z) - L_f F] \; + \; \frac{\Delta t}{C_s\rho_s \Delta z}$$

$$[\varepsilon_s (R_L\downarrow - \sigma T_{n,1}^4) - H - LH] \; + \; T_{n,1} \qquad (3)$$

Subscript $n$ denotes the time step and subscript $i$ denotes the snow layer; $i = 1$ denotes the snow surface in contact with air, $C_s, \rho_s, \lambda_s$ and $\varepsilon_s$ are respectively the specific heat capacity, density, conductivity and emissivity of snow; $\mu$ is the extinction coefficient of

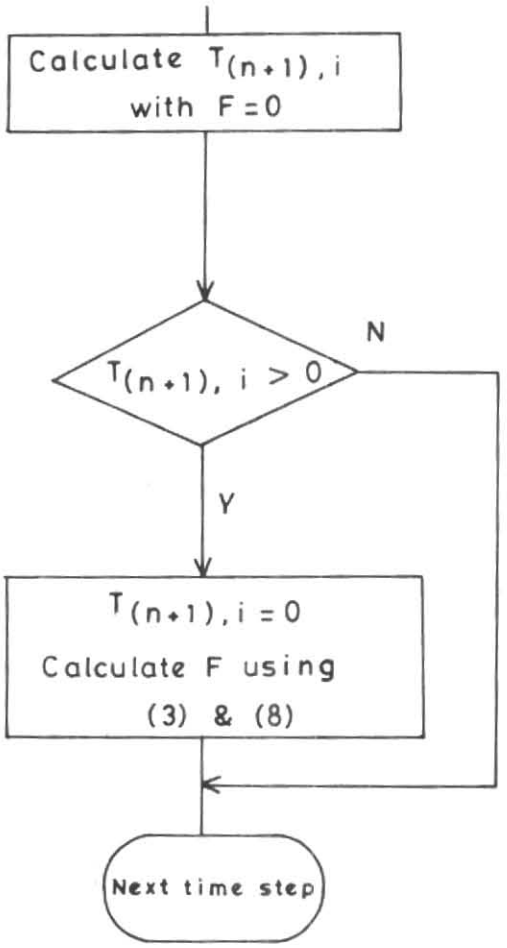


**Fig. 1.** Algorithm used for calculating snowmelt rate F [Kondo and Yamazaki (1990)]

solar radiation within the snow cover, $I$ [$= (1-\alpha)R_s$ ] and $R_L\downarrow$ are respectively the incident shortwave and longwave radiation at the snow surface, $\alpha$ is surface albedo of snow, $L_f$ is the latent heat of fusion of snow, $\sigma$ is Stefan- Boltzmann constant. $F$ is the amount of snowmelt per unit time and unit volume. The sensible heat flux ($H$) and latent heat flux ($LH$) are given by the following bulk relations :

$$H = C_p \rho C_H V_a (T_s - T_a) \quad (4)$$

$$LH = L_v \rho C_E V_a (q_s - q_a) \quad (5)$$

$C_H$ and $C_E$ are the drag coefficients, $L_v$ is the latent heat of vaporization and $C_p$ is the specific heat of air at constant pressure. Subscript '$a$' denotes ambient air values. During nights, considerable discrepancies were noticed in the simulated results. Hence during nights, the $T_s$ was found from ambient air temperature ($T_a$) using the following regression relations given by Upadhyay *et al.* (1981) for Kashmir.

$$T_s = 0^\circ \quad \text{if } T_a > -1^\circ C$$

$$T_s = 0.85 + 0.91\, T_a \quad \text{if } -3^\circ C \le T_a \le -1^\circ C$$

$$T_s = 1.75 + 0.65\, T_a \text{ if } T_a < -3^\circ C \quad (6)$$

The above regression relations were developed based on Kashmir valley observations only. Thus, these are valid in our study.

### 3.2. *Temperature stratification within the snow pack*

The temperature $T$ with in the snow pack is predicted by the following equation,

$$C_s \rho_s \frac{\partial T}{\partial t} = \lambda_s \frac{\partial^2 T}{\partial z^2} + \mu I \exp(-\mu z) - L_f F \quad (7)$$

Here, the first term on the right hand side (RHS) represents the heat conduction through the snow pack. The second term on RHS represents the absorption of solar radiation in the snow layer as given by Beer's law. Since the amount of solar radiation received by each snow layer is different, the melt rate $F$ was calculated for each of the snow layers. The temperature of the layers inside the snow pack was calculated by the following differential form of Eqn. (7).

$$T_{n+1,i} = \frac{\lambda_s \Delta t}{C_s \rho_s (\Delta z)^2} (T_{n,i-1} - 2T_{n,i} + T_{n,i+1}) + \frac{\Delta t}{\rho_s C_s} \left[ \mu I \exp(-\mu z) - L_f F \right] + T_{n,i} \quad (8)$$

$F$ is found using the algorithm given in Fig.1. $F$ is positive during melting and negative while freezing.

### 3.3. *Shortwave and longwave radiation*

The shortwave and longwave radiation terms were modified accounting for the effect of cloud cover in the model. Thus shortwave radiation was calculated by the empirical relation used by Adhikari and Ravishankar (1985) and Upadhyay *et al.* (1986) in their snow melt studies in Simla and Kashmir respectively, *viz.*,

$$R_s = R_o \left[1 - (0.82 - 0.000073\, z_c)\, N\right] \quad (9)$$

where, $R_o$ is the solar radiation received at the top

of the atmosphere, $z_c$ is the cloud height in metres and $N$ is the cloud amount in decimal fraction. $z_c$ and $N$ were taken from synoptic observations.

The net longwave radiation is modified as follows (Oke 1978):

$$R_L \text{ Net} = R_L \text{ Net (clear)} \ (1 - bN^2) \qquad (10)$$

where, $R_L$ Net and $R_L$ Net (clear) represent the net longwave radiation at a snow surface under cloudy and clear sky conditions respectively. Constant $b$ depends on the observed cloud type and cloud height. The values of $b$ are given by Oke (1978). $b$ was chosen to have the value of 0.88. This empirical formulation [Eqn. (10)] with constant '$b$' was used in several studies. For example, Segal *et al.* (1986) have studied with this formulation. Several other formulations, such as Brunt (1932), Swinkbank (1963) & Idso and Jackson (1969) were tried and these were found to be not applicable to Kashmir region studied here.

## 4. Methodology

In this study, the temporal variations of $u$, $v$, $\theta$ and $q$ in the atmosphere were calculated by the set of Eqns. (1). The snow surface temperature was calculated by Eqn. (2) using auxilliary Eqns. (4) & (5). The regression relations of Eqn. (6), were used to correct the snow surface temperature during night. The cloud cover effects on the incoming/outgoing, short/longwave radiations were included in the computations through Eqns. (9) & (10). Since snow surfaces are translucent to the incoming solar radiation, separate computations were necessary to calculate the temperature at snow surface and inside the snow pack. The temperature inside the snow pack was calculated using Eqn. (7). Thus Eqns. (2) & (7) are complimentary equations and not contradictory. The relevant differential equations were solved using finite difference method. As example, finite differencing of Eqn. (2) is given as Eqn. (3). The vertical exchange coefficient ($K_z$) in Eqn. (1) was calculated in the surface layer using similarity theory relations. Above the surface layer, $K_z$ was calculated as a function of local atmospheric stability ($R_i$) using Blackadar (1979)'s analytical formulation. Modified Crank-Nicolson method was used to solve the diffusion part of Eqn. (1). Additional details can be seen in Pielke (1984).

**TABLE 1**

**Model parameters**

| | |
|---|---|
| $\Delta t$ = 600 s | $C_s$ = 0.5 cal gm$^{-1}$ deg$^{-1}$ |
| $\Delta z_s$ = 2 cm | $\rho_s$ = 0.8 gm cm$^{-3}$ |
| $\varepsilon_s$ = 0.82 | $\alpha$ = 0.8 |
| $Z_0$ = 0.01 cm | $\lambda_s = 4 \times 10^{-4}$ cal cm$^{-1}$ s$^{-1}$ deg$^{-1}$ |
| $F_w$ = 0.1 | $\mu$ = 0.4 cm$^{-1}$ |

## 5. Initial data and boundary conditions

Simulations were carried out by initializing the 1-D model with RS/RW data reported at Srinagar (34° 05'N, 74° 50' E; altitude 1585 m amsl) in Kashmir valley. Simulations were started at local sunset with an isothermal snow pack. In the atmosphere, 11 levels were taken in the vertical at unequal grid intervals. The model top was at 4000 m. 11 levels at equal grid intervals ($\Delta z_s$) of 2 cm were taken within the snow pack. Results obtained using 12 UTC data of two synoptically calm days with ground snow cover, *viz.*, 13 January 1968 and 5 February 1980 are presented here. The simulations were performed on the days following fresh snow fall. During synoptically disturbed period on snow days the model yielded computationally unstable solutions. Hence, simulations were performed only on days after cessation of snow fall. In addition, some results obtained using February 1978 monthly mean data are also shown.

At the lower boundary ($z = z_0$),

$$u = v = 0; \ q_s = q_{sat} \ F_W + (1 - F_w) \ q(1)$$

where, $q_s$ and $q(1)$ are the specific humidity at the snow surface and 1st level of the model respectively; $z_0$ is the roughness length of snow, $q_{sat}$ is the saturated value of humidity and $F_W$ is the degree of wetness.

At the model top ($z = H$ = 4 km),

$u = U_g$ and $v = V_g$ , $\theta(H)$ = constant, $q(H)$ = constant.

$\theta(H)$ and $q(H)$ at $H$ = 4 km (top of the model) were specified from synoptic observations for the simulated days. The top of the model was fixed by trial and error method so that there were no boundary effects felt below this.

## 6. Results and discussion

Model simulations were carried out with a time step ($\Delta$ t) of 600 seconds with the input parameters given in Table 1. The initial potential temperature ($\theta$), specific humidity ($q$) and wind speed ($v$) profiles taken at Srinagar (Kashmir valley) for 13 January 1968 and 5 February 1980 are shown in Figs. 2(a-d). It is

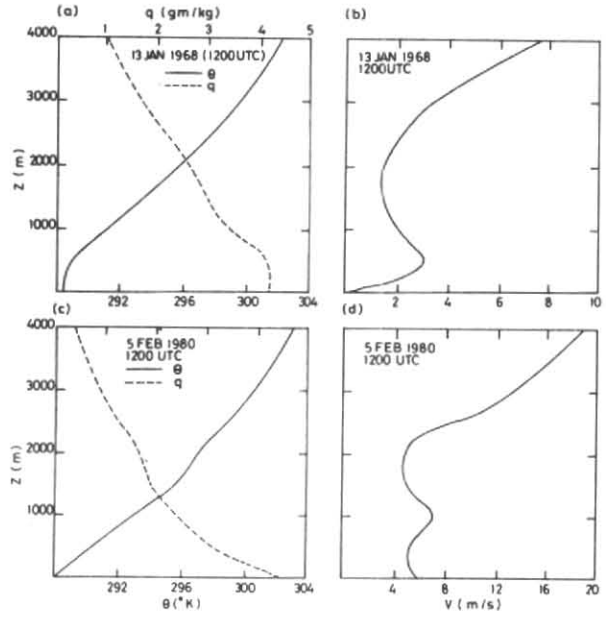


**Figs. 2(a-d).** Initial (a & c) potential temperature (θ) and specific humidity ($q$) profiles and (b & d) wind speed ($V$) profiles at Srinagar, Kashmir valley

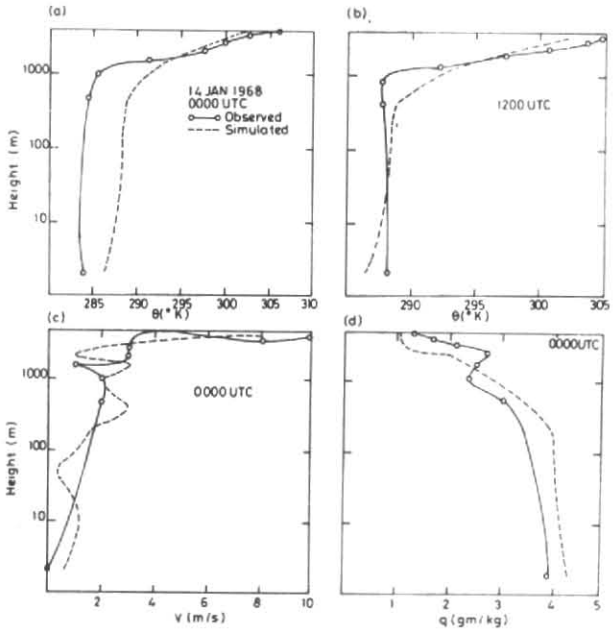


**Figs. 3(a-d).** Model-simulated θ profiles at (a) 00 UTC and (b) 12 UTC & (c) wind speed ($V$) profiles and (d) specific humidity ($q$) profiles at 00 UTC (13 January 1968 data) compared with observations

necessary to note that the observational curves given in the diagrams are based on Srinagar RS/RW observations taken in Srinagar at standard pressure levels, which are widely spaced. For comparison and for computations, linearly interpolated observational values were used in the absence of fine resolution data. Since all such approximations are artificial, one can not expect one-to-one coincidence with the numerical simulated values.

Some of the model simulated results obtained for 13 January data are shown alongwith observations in Figs. 3 (a-d). At 00 UTC, *i.e.*, after 12 hours of simulation, the model-simulated θ values are found to over-estimate by about $2^{\circ}$ $K$ upto 1 km (Fig. 3a). However, better θ profiles were obtained after 24 hours of simulation as shown in Fig. 3(b). During night hours, the snow surface temperature was determined using the regression relations [Eqn. (6)]. This was necessitated by the large radiational cooling of the snow surface, especially during nights with insufficient compensation provided by the convective heat transfer from the atmosphere. In real atmosphere, however, enough heat is convectively transferred by the turbulent fluxes to offset the net emission of radiation during nights. The "bursts" of turbulence which often offset the radiative balance of snow surface, as pointed out by Halberstam and Melendez (1979), cannot be amply parameterized by current surface layer theory.

The model-simulated wind speed profiles were found to be in reasonable agreement with observations. Fig. 3(c) shows the comparison of model-simulated wind speed profiles with observations at 00 UTC. In Fig. 3(c), the sharp turning points denote shear zones that are usually present in stable atmosphere. These shear zones are believed to be responsible for the mixing of warmer air from above with colder air below it in highly stable atmosphere. Since special observations were not taken during the periods of our study, these are absent in observational curves. The model predicted specific humidity profile ($q$) compared with observations at 00 UTC in Fig. 3(d) shows a fair agreement with observations. The 12 UTC $q$ profile also reveals the same, which is not shown here for brevity.

Melting of snow occurred during daytime in the snow layers whose temperature exceeded $273^{\circ}$K. Since snow temperature cannot exceed $273^{\circ}$K, it was set back to $273^{\circ}$K allowing the excess heat to go for melting (see Fig. 1). Due to the penetration of solar radiation into the snow pack, internal melting occurred. Interestingly, melting started inside the snow pack after sunrise while the snow surface in contact with the atmosphere was still below $273^{\circ}$K. This is because of the domination of the outgoing longwave radiation at the snow surface with slow compensation of heat from the inside layers of the snow pack due to the poor

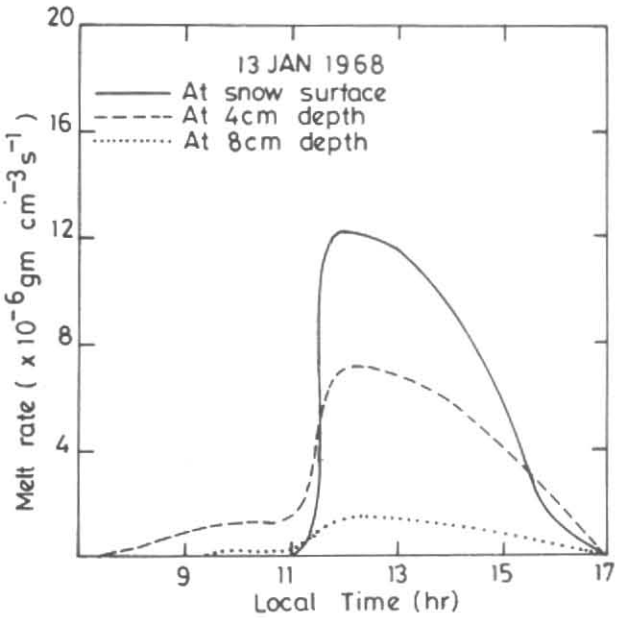


Fig. 4. Temporal variation of snowmelt rate ($F$) at snow surface and at depths 4 and 8 cm inside the snow pack (13 January 1968 data)

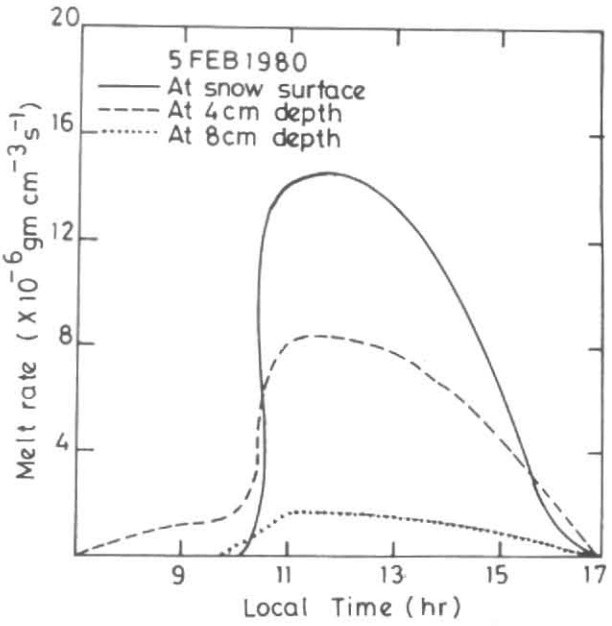


**Fig. 5. Same as Fig. 4 but for February data**

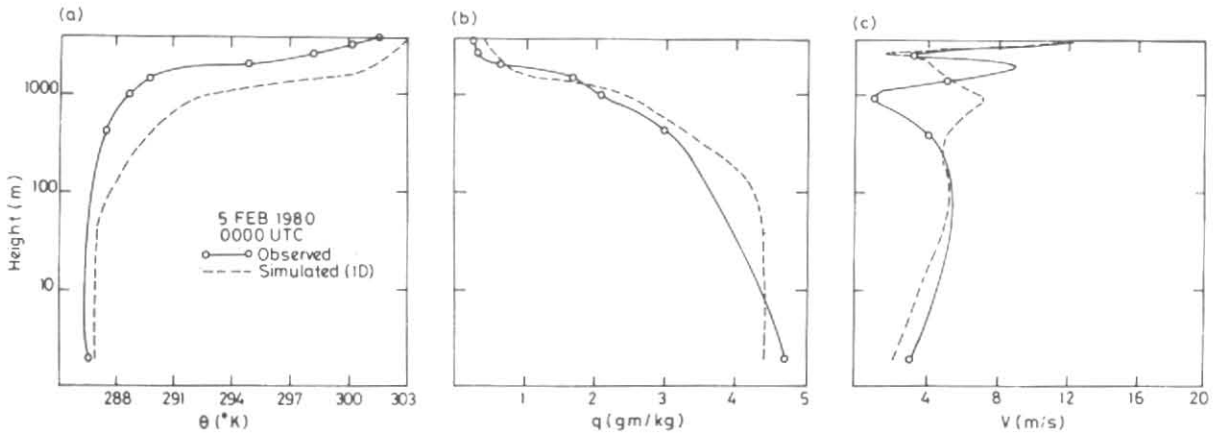


Figs. 6(a-c). Comparison of model-simulated (a) θ - profile, (b) specific humidity ($q$) profiles and (c) $V$ profiles compared with observations at 00 UTC (5 February 1980)

thermal conductivity of snow. But about 3 hours after sunrise (*i.e.*, at ~ 1000 LST), the incoming solar radiation was sufficient to heat the snow surface resulting in an increase in its melt rate. Fig. 4 shows the temporal variation of snow melt rate at the surface, 4 cm depth and at 8 cm depth inside the snow pack for the first 24 hours. Maximum melt rates were obtained at noon. A maximum value of ~ $12 \times 10^{-6}$ gm $cm^{-3}$ $s^{-1}$ was obtained at the surface which decreased with depth. This is due to the exponential decrease in the amount of solar radiation absorbed by the different snow layers as given by Beer's law (see section 3).

Simulations obtained with 5 February 1980 data are also compared with observations. Figs. 6(a-c) show these comparisons at selected hours. Fig. 6(a) shows the model-simulated potential temperature (θ) profiles compared with observations at 00 UTC. The model simulations agree well with observations in the lower atmosphere. But above 400 m, the model-simulated values overestimate by about 3-4°K. The model-simulated $q$ profile for the corresponding hour is found to be in good agreement with the observed profiles as seen in Fig. 6(b). The model simulated $V$ profiles at 00 UTC were in better agreement with observations

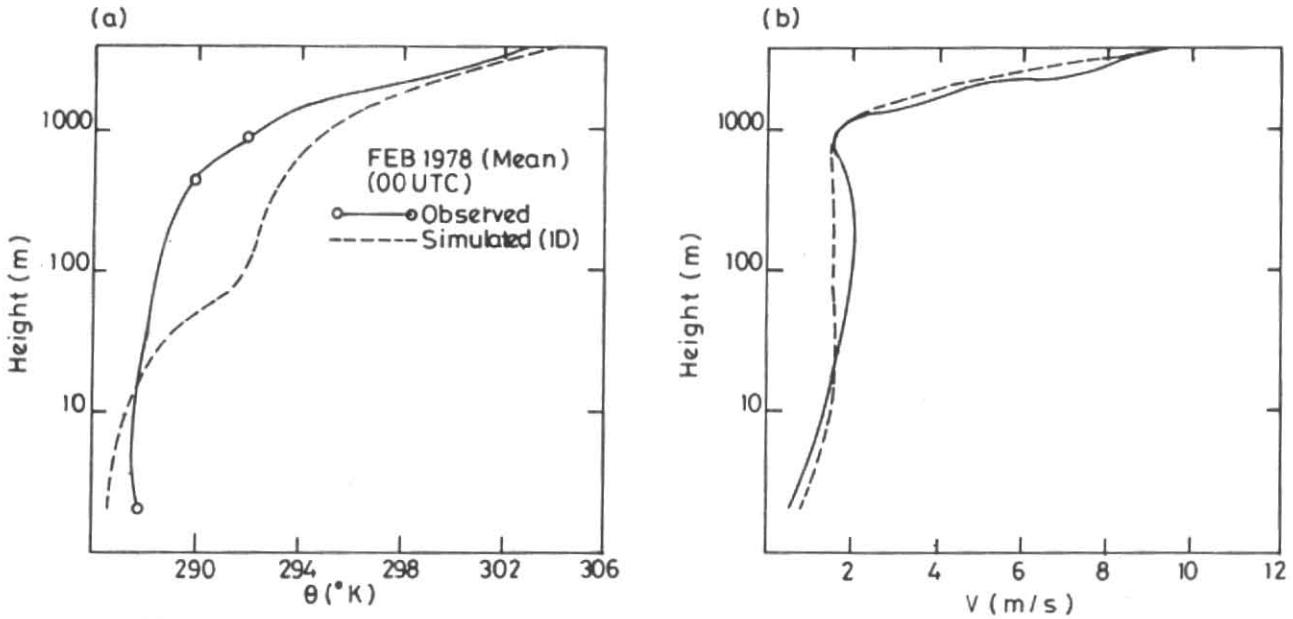


Figs. 7(a&b). Comparison of model-simulated (a) θ - profiles and (b) $V$-profiles with observation at 00 UTC (February 1978 mean data)

**TABLE 2**

**Comparison of model-simulated θ, q and V values at 00 UTC (13 January 1968 data) with different drag coefficients**

| Z (m) | $C_D = 2.0 \times 10^{-3}$ | | | $C_D = 1.5 \times 10^{-3}$ | | |
|---|---|---|---|---|---|---|
| | θ (°K) | $q$ (g kg$^{-1}$) | $V$ (ms$^{-1}$) | θ (°K) | $q$ (g kg$^{-1}$) | $V$ (ms$^{-1}$) |
| 2 | 276.6 | 2.3 | 0.4 | 277.8 | 2.5 | 0.6 |
| 10 | 278.6 | 2.6 | 0.9 | 278.9 | 2.6 | 0.9 |
| 20 | 281.6 | 3.2 | 1.1 | 281.4 | 3.2 | 1.1 |
| 50 | 285.4 | 4.0 | 1.4 | 285.3 | 4.1 | 1.4 |
| 100 | 286.7 | 4.2 | 0.9 | 286.7 | 4.2 | 0.9 |
| 200 | 287.7 | 4.0 | 2.1 | 287.7 | 3.9 | 2.1 |
| 500 | 288.7 | 3.3 | 3.0 | 288.7 | 3.3 | 3.0 |
| 1000 | 291.1 | 2.4 | 2.0 | 291.9 | 2.4 | 2.0 |
| 2000 | 295.6 | 1.7 | 1.4 | 295.6 | 1.7 | 1.4 |
| 3000 | 299.4 | 1.1 | 3.3 | 299.4 | 1.1 | 3.3 |
| 4000 | 302.2 | 1.0 | 7.9 | 302.2 | 1.0 | 7.9 |

(see Fig. 6c). However, the model simulated values at 12 UTC (not shown here) were in poor agreement with observations due to the rapid synoptic scale fluctuations during this period.

For this data also, the melting behaviour of the snow layers was found to be similar to January data with maximum melting occurring at the snow pack surface and decreasing with depth (see Fig. 5). The maximum melt rate obtained was ~ $15 \times 10^{-6}$ gm cm$^{-3}$ s$^{-1}$ showing higher melt rate in February than in January. The incoming/outgoing short and longwave radiations were corrected for cloud cover effects in computations using Eqns. (9) & (10). Snow melt rates were determined only with cloud cover. This is expected because the amount of insolation received in February is more than in January. An average melt rate of 0.36 and 0.54 cm day$^{-1}$ were obtained respectively for January and February. For verification purpose, melt rate was also calculated using the following standard empirical formulation which was also used by Upadhyay (1994) in his study of snowmelt processes, *viz.*,

$$M = (0.029 + 0.0084\ V)\ (T - 32\ ) + 0.09 \quad (11)$$

where, $M$ is the melt rate (inches day$^{-1}$), $V$ is the wind speed (mph) and $T$ is the air temperature (°F). Using this formulation, the snowmelt values obtained for January and February were 0.23 and 0.5 cm day$^{-1}$ respectively. The difference between model-simulated melt rates and computed values by empirical relation given above could be due to the empirical constants, which can vary depending upon the geographical location. In heat or mass transfer studies, such variations are common. It is necessary to note that the order of magnitudes remain the same.

Simulations using February mean data were compared with observations. Typical results are shown in Figs. 7 (a & b). As 00 UTC (Fig. 7a), the model

simulated θ values are found to be more closer to observations in the lower levels of the atmosphere. At higher levels, the model-simulated values were found to be higher by about 3-4° K. The model simulated wind speed profiles are in good agreement with observations as could be seen from Fig. 7(b) which shows the profiles at 00 UTC. The values of the drag coefficients $C_D, C_H$ depend on the roughness of the terrain. They range from about $10^{-3}$ for ocean and smooth surfaces to about $3 \times 10^{-3}$ over rough terrain (Washington and Parkinson 1986). Sensitivity tests were conducted for different values of $C_D$. The results given in Table 2 show that they are insensitive to change in drag coefficient values except at $z = 2$ m, which is within the surface layer. Hence, a constant value of $2 \times 10^{-3}$ was used for the drag coefficients. Since no precipitation was reported on the days chosen, precipitation scheme was not included in the present study.

## 7. Conclusions

Numerical simulations were performed using RS/RW data reported at Srinagar. Suitable modifications were incorporated in the mesoscale model for the simulation of atmospheric variables with ground snow cover for a full diurnal cycle. The simulated atmospheric variables were in reasonable agreement with observations despite being a 1-D simulation. Penetration of solar radiation into the snow pack led to melting of the inside layers, the melt rate decreasing with depth. There was a time lag of about three hours before the onset of melting at the snow pack surface compared to its inside layers. An average melt rate of 0.36 and 0.54 cm $day^{-1}$ was obtained for January and February respectively. These values compared well with the values calculated using standard empirical formulation. A more detailed verification is possible only with the availability of systematic observations for snow melt rate, diurnal variation of snow temperature, etc.

*Acknowledgements*

This study was supported by a research grant (DST No. ESS/CA/B2-002/90) of Department of Science and Technology, Government of India. The compu- tations were performed using ICL 3980 system at IIT, Delhi.

### References

Adhikari, R.N. and Ravishankar, A.D., 1985, "Snowmelt run-off modelling using Landsat imagery-A Pilot study", *Vayu Mandal*, **15**, 1&2, 50-54.

Anderson, E.A., 1976 "A point energy and mass balance model of a snow cover", NOAA Tech. Report NWS 19, U.S. Dept. of Commerce, 150 p.

Blackadar, A.K., 1979, "High resolution models of the planetary boundary layer", *Adv. Environ. Sci. Engg.*, **1**, 50-85.

Brunt, D., 1932, "Notes on radiation in the atmosphere", *Quart. J. Roy. Meteorol. Soc.*, **58**, 389-420.

Granger, R.J. and Male, D.H., 1978, "Melting of a prairie snow pack," *J. Appl. Meteor.*, **17**, 1833-1842.

Halberstam, I. and Melendez, R., 1979, "A model of the planetary boundary layer over a snow surface", *Bound. layer. Meteor.*, **16**, 431-452.

Idso, J. and Jackson, R.D., 1969, "Thermal radiation from the atmosphere", *J. Geophy. Rev.*, **74**, 5397-5403.

Kahle, A.B., Schieldge, J. and Paley, H.N., 1977, "JPL field measurements at the finney country, cansdas, test site, October 1976", JPL publication, 77-1, Pasadena, CA, 62 p.

Kondo, J. and Yamazaki, T., 1990 "A prediction model for snowmelt, snow surface temperature and freezing depth using a heat balance method", *J. Appl. Meteor.*, **29**, 375-384.

McKay, D.C. and Thurtell, G.W., 1978, "Measurements of the energy fluxes involved in the energy budget of a snow cover", *J. Appl. Meteor.*, **17**, 339-349.

McNider, R.T. and Pielke, R.A., 1981, "Diurnal boundary layer development over sloping terrain", *J. Atmos. Sci.*, **38**, 2198-2212.

Mahrer, Y. and Pielke, R.A., 1977, "A numerical study of the air flow over irregular terrain", *Contrib. Atmos. Phys*, **50**, 98-113.

Ohata, T., Higuchi, K. and Ikegami, K., 1981, "Mountain-valley wind system in the Khumu Himal, East Nepal", *J. Meteor. Soc. Japan.*, **59**, 5, 753-762.

Oke, T.R., 1978, "Boundary layer climates", Methuen & Co. Ltd., London, 372 p.

Pielke, R.A., 1974, A "three-dimensional numerical model of the sea breezes over south Florida", *Mon. Wea. Rev.*, **102**, 115-139.

Pielke, RA., 1984, "Mesoscale Meteorological Modelling", Acad. Press, 612 p.

Schubert, J.F., 1977, "Acoustic reduction of momentum transfer during the abrupt transition from a laminar to turbulent atmospheric boundary layer", *J. Appl. Meteorol.*, 16, 1292-1297.

Segal, M., Purdom, J.F.W., Song, J.L., Pielke, R.A. and Mahrer, Y., 1986, "Evaluation of cloud shading effect on the generation and modification of mesoscale circulations", *Mon. Wea. Rev.*, **114**, 1201-1212.

Swink bank, W.C., 1963. "Longwave radiation from clear skies", *Quart. J. Roy. Meteorol. Soc.*, **89**, 339-348.

Upadhyay, D.S., 1994, "Snowmelt processes and applications", *Mausam*, **45**, 2, 129-138.

Upadhyay, D.S., Kathuria, S.N. and Kaur, S., 1986, "Impact of snow cover on monsoon fluctuation", Basic physics of monsoon, DST report, 112 p.

Upadhyay D.S., Rajnikant and Rao, D.V.L.N., 1981, "A study on heat transfer in seasonal snowpack", *Mausam*, **32**, 4, 411-414.

Washington, W.M. and Parkinson, C.L., 1986, "An introduction to three dimensional climate modelling", Oxford Univ. Press, New York, 422 p.